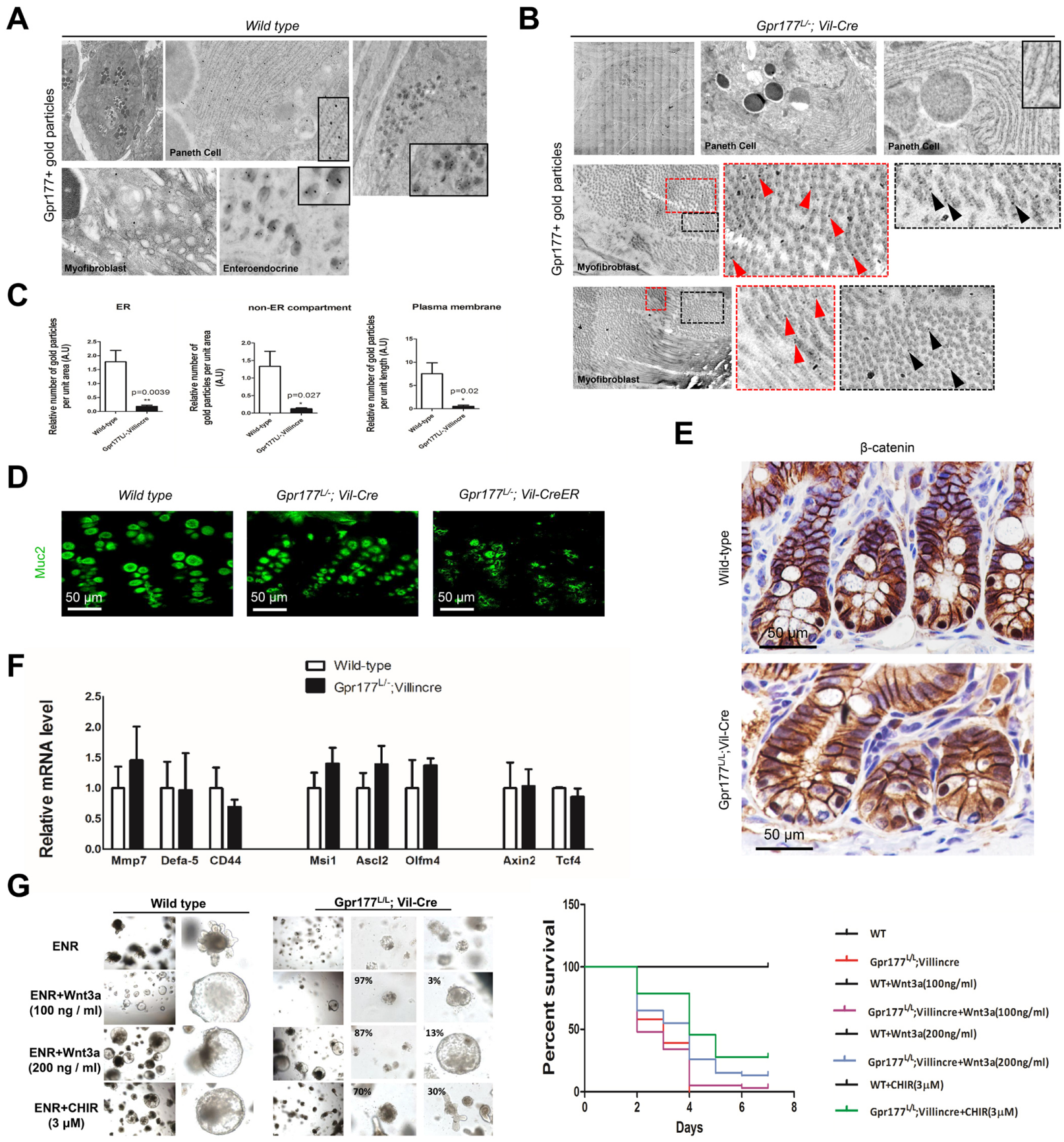

Fig. S1. (A) Transmission electron microscopy (TEM) revealed presence of Gpr177+ immunogold particles in intestinal epithelial cells, specifically Paneth cells and enteroendocrine cells, and myofibroblasts in wild type intestines. (B) TEM showed reduction in the number of Gpr177+ immunogold particles in the Paneth cells of *Gpr177$^{L/-}$;Vil-Cre* intestines while there was no change in the immunogold particle numbers in the stromal cells (red and black arrowheads). (C) Number of Gpr177+ colloidal gold particles quantified in ER, non-ER (Golgi/vesicle) and plasma membrane along with the area (ER and non-ER) or perimeter (plasma membrane) covered by each compartment in wild-type and *Gpr177$^{L/-}$; Vil-Cre* Paneth cells.
(D) Muc2 staining of wild type, *Gpr177$^{L/-}$;Vil-Cre*, and *Gpr177$^{L/-}$;Vil-CreER* mouse colons.
(E) Immunostaining showed that number of nuclear β-catenin positive cells was not changed between wild type and *Gpr177$^{L/L}$;Vil-Cre* mouse small intestinal crypts.
(F) Quantitative RT-PCR showed no change in ISC (Msi1, Ascl2, Olfm4, Axin2, and Tcf4)and Paneth cell (Mmp7, Defa-5, and CD44) signature genes in *Gpr177$^{L/-}$;Vil-Cre* mouse intestines. N=3 for each genotype.
(G) Enteroids were grown from ileal crypts of wild type and *Gpr177$^{L/L}$;Vil-Cre* mice, cultured in ENR or ENR supplemented with Wnt3a (100 ng/ml or 200 ng/ml) or CHIR (3 µM). *Gpr177$^{L/L}$;Vil-Cre* mouse enteroids failed to grow in ENR medium. The bolded percentage for *Gpr177$^{L/L}$;Vil-Cre* mouse enteroids indicates the population of organoids similar to the representative image. Exogenous Wnt3a (200 ng/mL, blue line) and CHIR (green line) enhanced survival of a fraction of Gpr177$^{L/-}$;Vil-Cre mouse enteroids.

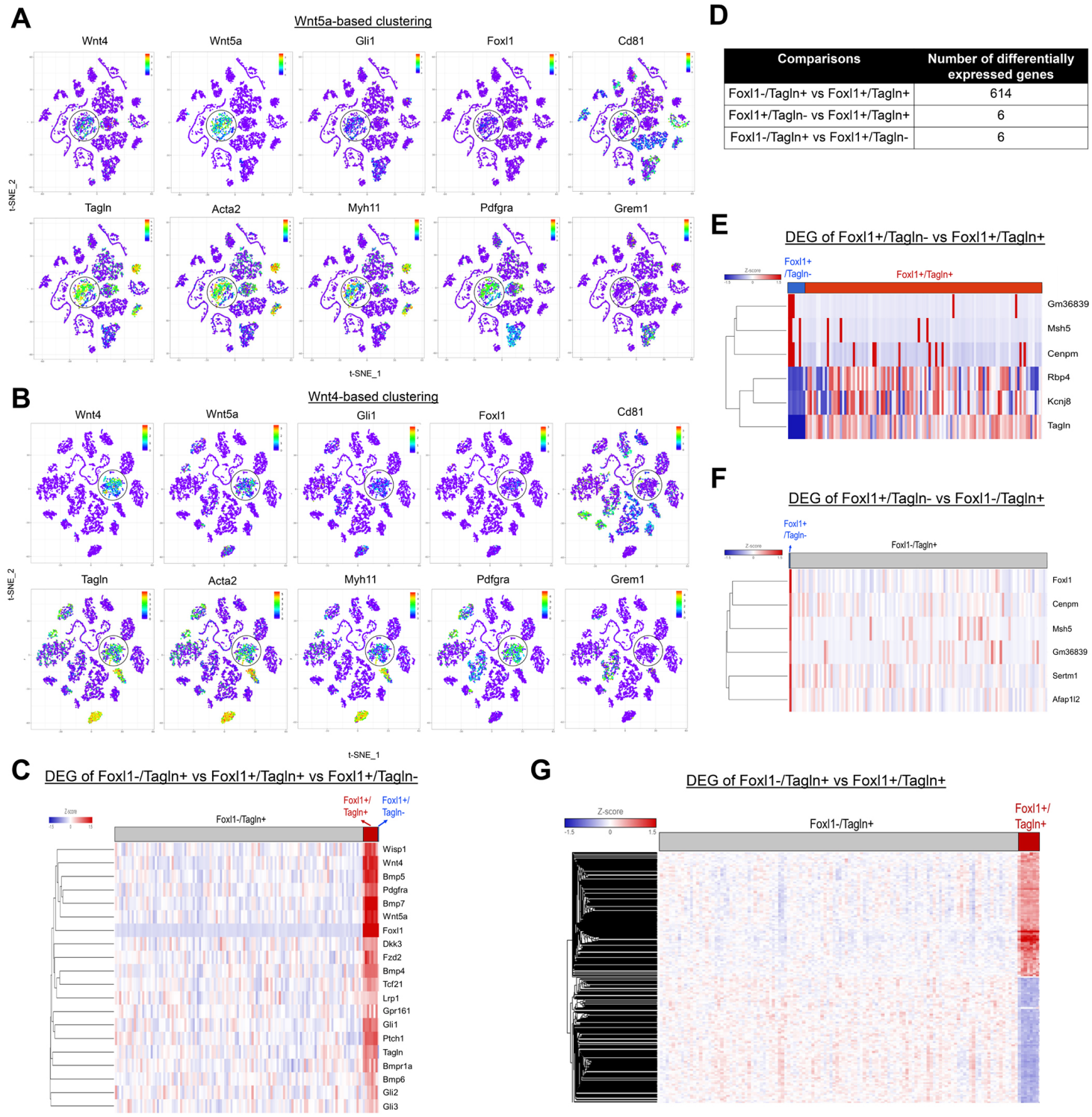

Fig. S2. (A) t-SNE plot of Wnt5a-based Single Cell Deep Constrained Clustering (scDCC) of the mouse ileal stromal cells. Wnt5a-expressing cells (circled in black) highly co-expressed Wnt4, Tagln, Acta2, Pdgfra, and Myh11.

(B) t-SNE plot of Wnt4-based scDCC clustering of the mouse ileal stromal cells. Wnt4-expressing cells (circled in black) highly co-expressed Wnt5a, Tagln, Acta2, Pdgfra, and Myh11.

(C) Heatmap of the transcriptomes of Tagln+/Foxl1-, Tagln+/Foxl1+, and Tagln-/Foxl1+ populations indicated a Foxl1-driven expression change in Tagln+/Foxl1+ cells.

(D) Table summarizing the number of differentially expressed genes between Foxl1-/Tagln+ and Foxl1 +/Tagln+, Foxl1+/Tagln- and Foxl1+/Tagln+, Foxl1-/Tagln+ and Foxl1+/Tagln- populations. (E) Heatmap showed relative expression of the 6 genes differentially expressed between Foxl1+ /Tagln- and Foxl1+/ Tagln+ populations.

(F) Heatmap showed the relative expression of the 6 genes differentially expressed between Foxl1-/ Tagln+ and Foxl1+/Tagln- populations.

(G) Heatmap showed relative expression of the 614 differentially expressed genes detected between Foxl1-/Tagln+ and Foxl1+/Tagln+ populations.

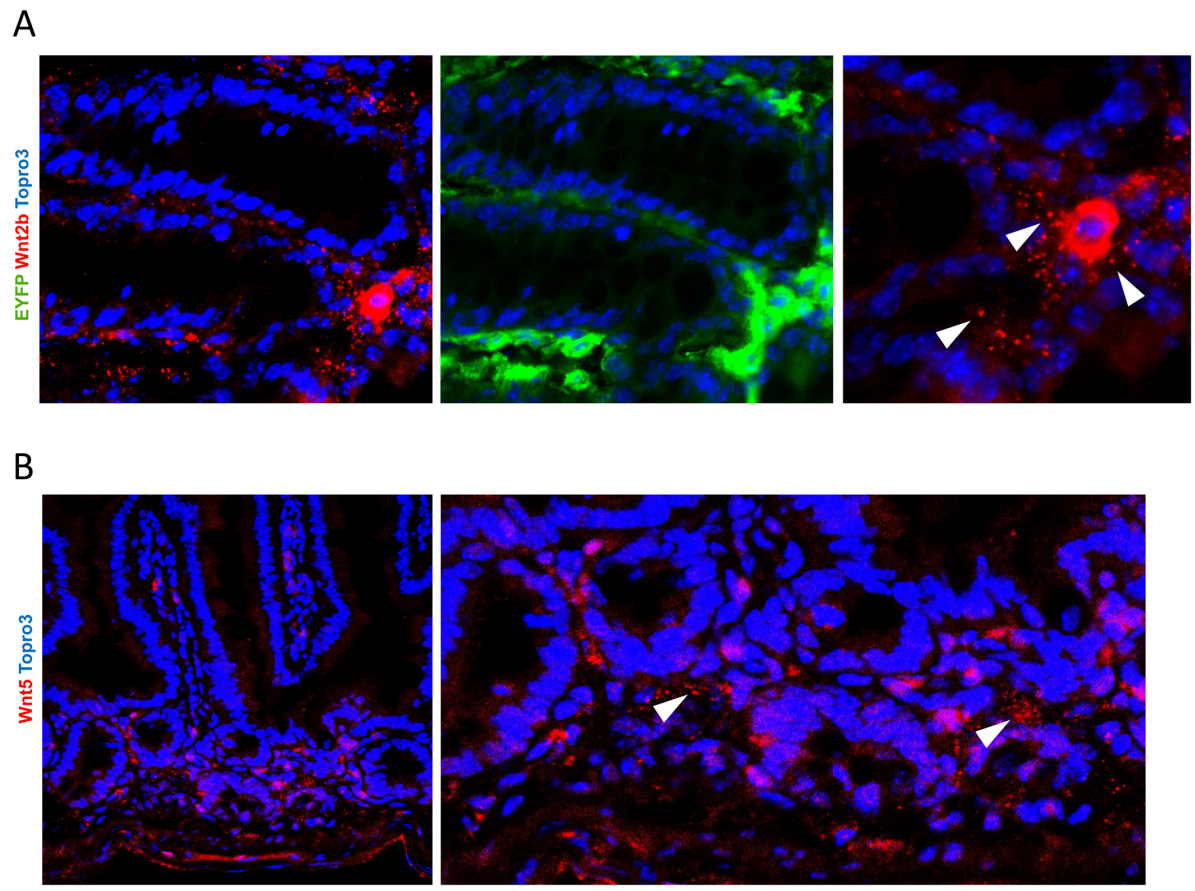

Fig. S3. (A) Co-staining of Wnt2b with EYFP in *Tagln-Cre; Rosa26R-EYFP* mouse colons showed Cre-activated reporter expression in Wnt2b+ cells (white arrowheads).
(B) Staining of Wnt5 in *Tagln-Cre; Rosa26R-EYFP* mouse small intestines revealed perinuclear and vesicular localization of Wnt5 (white arrowheads).

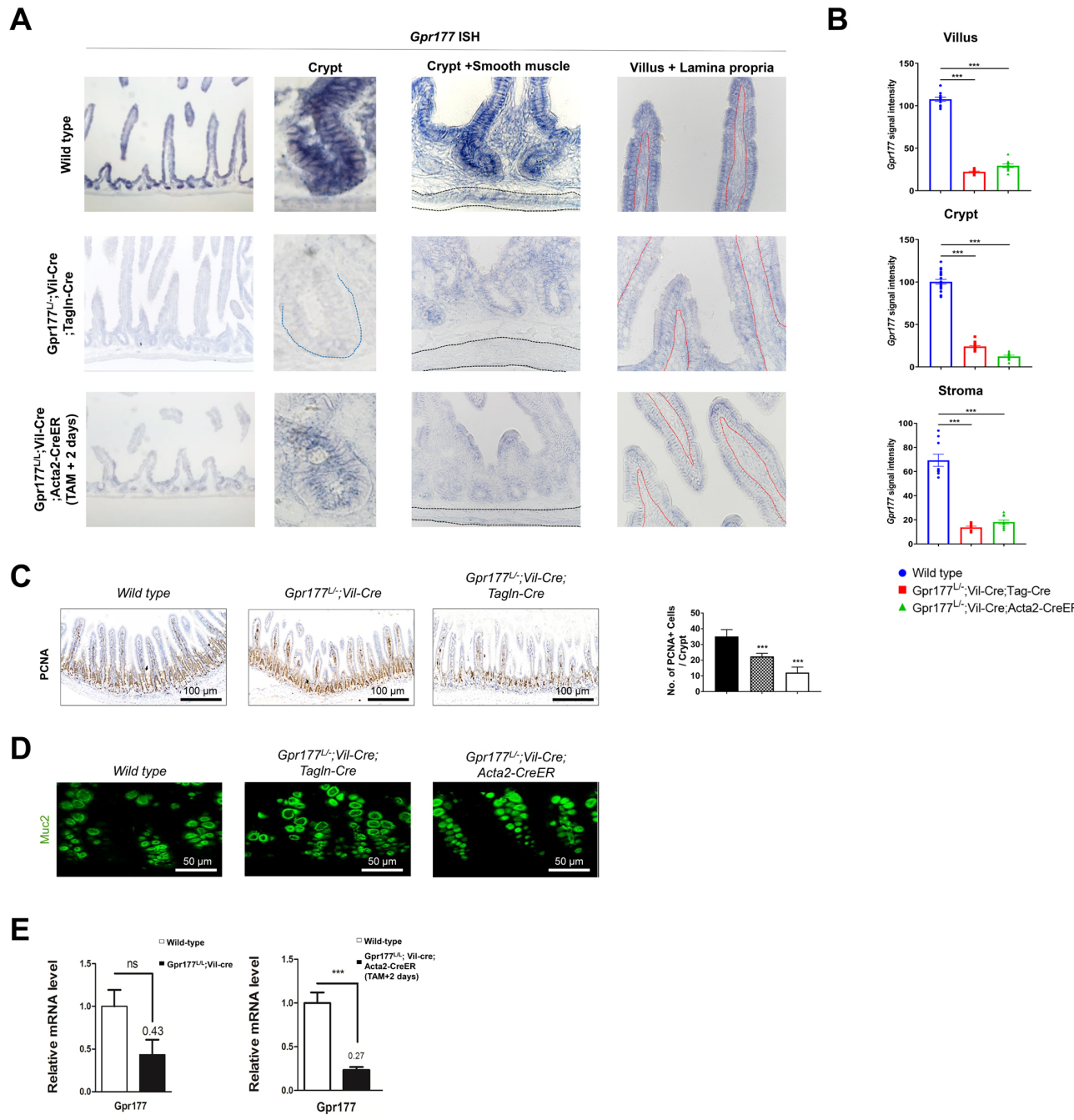

Fig. S4. (A-B) RNA *in situ* hybridization of Gpr177 revealed significant deletion in villus, crypt, and stromal cells of *Gpr177$^{L/-}$;Vil-Cre;Tagln-Cre* and *Gpr177$^{L/L}$;Vil-Cre;Acta2-CreER* mice. The blue dotted line delineates the crypt, black dotted lines delineate smooth muscles, and red dotted lines delineate the lamina propria.
(C) Immunohistochemistry of PCNA showed reduction in numbers of proliferating cells in *Gpr177$^{L/L}$;Vil-Cre* and *Gpr177$^{L/-}$;Vil-Cre;Tagln-Cre* mice.
(D) The number of Muc2+ cells were unchanged between wild type, *Gpr177$^{L/-}$;Vil-Cre;Tagln-Cre* and *Gpr177$^{L/-}$;Vil-Cre;Acta2-CreER* mouse colons.
(E) RT-PCR of Gpr177 showed no change between wild type and *Gpr177$^{L/L}$;Vil-Cre* intestines while there was a significant reduction in *Gpr177$^{L/L}$;Vil-Cre;Acta2-CreER* intestines compared to wild type

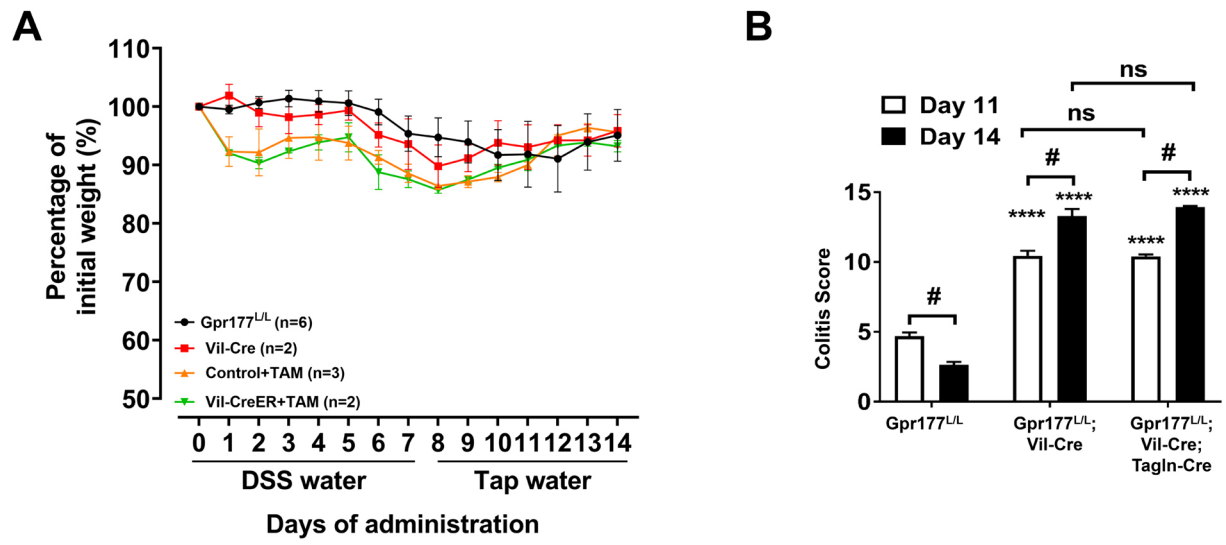

Fig. S5. (A) Body weight analysis of control mice included Gpr177 flox/flox (no cre) littermates, as well as Vil-Cre only mice, and tamoxifen-injected WT and Vil-CreER mice (non-littermates), with indicated numbers, did not show any significant difference.
(B) Colitis scored by a different matrix consisting of ulceration, crypt death, immune cell infiltration, thickness of colonic wall, and loss of goblet cell showed increased pathological indexes in *Gpr177$^{L/L}$;Vil-Cre* and *Gpr177$^{L/L}$;Vil-Cre;Tagln-Cre* mice.

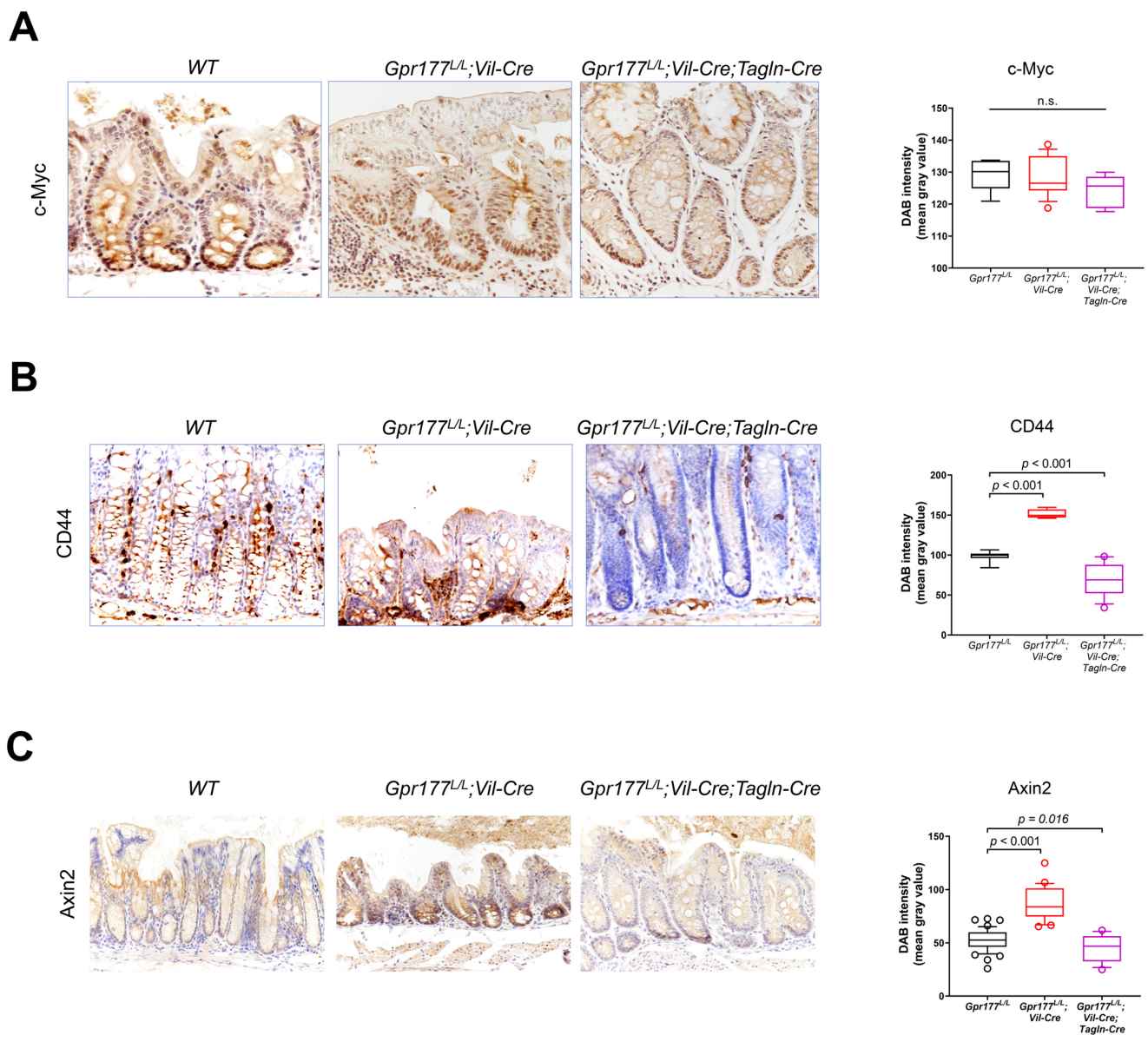

Fig. S6. (A) Immunohistochemistry and quantification of c-Myc in DSS-treated *Gpr177$^{L/L}$*, *Gpr177$^{L/L}$;Vil-Cre,* and *Gpr177$^{L/-}$;Vil-Cre;Tagln-Cre* mouse colons.

(B) Immunohistochemistry and quantification of CD44 in DSS-treated *Gpr177$^{L/L}$*, *Gpr177$^{L/L}$;Vil-Cre,* and *Gpr177$^{L/-}$;Vil-Cre;Tagln-Cre* mouse colons.
(C) Immunohistochemistry and quantification of Axin2 in DSS-treated *Gpr177$^{L/L}$*, *Gpr177$^{L/L}$;Vil-Cre,* and *Gpr177$^{L/-}$;Vil-Cre;Tagln-Cre* mouse colons.
Significance of differences was determined by two-tailed t test.

Table S1. Sequences of the quantitative RT-PCR primers

Gene	Forward	Reverse
Tcf4	AGCCCGTCCAGGAACTATG	TGGAATTGACAAAAGGTGGA
Axin2	TGAGATCCACGGAAACAGC	GTGGCTGGTGCAAAGACAT
Gpr177	CAAATCGTTGCCTTTCTGGT	CGCCAGCCATCTTGTTTTAT
Mmp7	CTTACAAAGGACGACATTGCAG	AGTGCAGACCGTTTCTGTGAT
Defa5	TATCTCCTTTGGAGGCCAAG	TTTCTGCAGGTCCCAAAAAC
CD44	CACCATTGCCTCAACTGTGC	TTGTGGGCTCCTGAGTCTGA
Ascl2	TCCAGTTGGTTAGGGGGCTA	GCATAGGCCCAGGTTTCTTG
Olfm4	GCCACTTTCCAATTTCAC	GAGCCTCTTCTCATACAC
β-actin	TTGCTGACAGGATGCAGAAG	CCACCGATCCACACAGAGTA
Hprt	AAGCTTGCTGGTGAAAAGGA	TTGCGCTCATCTTAGGCTTT